

# Simulation of the process chain from forming to crash taking into account stochastic aspects

Dong-Zhi Sun, Florence Andrieux

Fraunhofer Institute for Mechanics of Materials IWM, Woehlerstrasse 11, 79108 Freiburg

Markus Feucht

Daimler AG, W059 / HPC X271, 71059 Sindelfingen

## **Abstract:**

The local mechanical properties e.g. flow stress and fracture strain in an automotive component manufactured by deep drawing are inhomogeneous due to different local deformation degrees which affect the component behavior under crash loading. A reasonable approach for modelling the deformation and damage behavior of a component produced by deep drawing is a coupling between forming simulation and crash simulation. However, many questions are still open for this approach, e.g. how strong the crash behavior of a component depends on the manufacturing process and the applied modelling methods and which damage model should be used for an integrated simulation. Moreover, it is necessary to quantify the influence of additional stochastic scatter of material properties on the numerical prediction of component behavior for crashworthiness analysis. Until now there are few results in the literature about the application of an efficient stochastic analysis for modelling of a process chain.

In this work a basic model was developed for modelling the process chain from forming to crash. Deterministic and stochastic scatters of the material properties in a component of the steel ZStE340 were experimentally characterized. The influences of pre-strain and pre-damage caused by forming on the crash behavior of the automobile component were investigated. The influences of loading history and triaxiality on damage behavior were quantified. A general material model which describes anisotropy and damage was developed and implemented for forming and crash simulations. To validate the applied concept component tests under bending with superposed tension were performed and simulated. This basis model was used for a stochastic analysis based on the singular value decomposition (SVD) method.

## **Keywords:**

Damage model, crash simulation, forming simulation, process chain, material characterization, component tests, pre-deformation, anisotropy, stochastic aspects.

## 1 Introduction

It is a great problem in crashworthiness analyses that the local properties e.g. yield stress and fracture strain in a component change from position to position and from charge to charge. The predictions of crash simulation performed without taking into account the scatter of material data may contain a high risk concerning their reliability. Although scatters of material data and geometry deviations play a key role for the construction and crash safety evaluation, stochastic analyses are rarely used for crash simulations. On the basis of crash simulations the program LS-OPT and other commercial crash codes offer possibilities, to separate the deterministic variables from non-deterministic variables (bifurcation, not predicable variations) to identify the most influential factors and to perform stochastic analyses [1]. However, such stochastic analyses are conducted in most cases without considering robustness aspects due to missing information about scatter of material data and the requirement on high computer capacity. In the few published works [2] only geometry and flow stress were varied in the stochastic analyses and the damage of component was not modelled.

In the frame of this work the scatter of the material properties including damage behaviour in a component of a micro-alloyed steel was characterized and analysed. The process chain from deep drawing to crash was simulated with the same material model. The deterministic effects e.g. distribution of pre-strain and pre-damage after manufacturing were quantified by forming simulation and taken into account in the crash simulation. A damage model was developed to simulate the influence of pre-damage caused by manufacturing and loading path. To study the consequence of scatter of material data on crash simulation results component tests were conducted and simulated. The main task of this work is the development of a physically meaningful basic finite element model for a stochastic analysis which was performed at Fraunhofer SCAI on the basis of the singular value decomposition (SVD) method [3].

## 2 Characterisation of deformation and damage behaviour

The accuracy of simulation results strongly depends on both material data and material model. Therefore, a comprehensive experimental program was established and realised. The material under consideration is the micro-alloyed fine grain steel ZStE340 which is widely used due to its formability. The steel sheet with a thickness of 1.75 mm was characterized with experiments on different specimen types e.g. smooth, notched and biaxial tension specimens and shear specimens. Additionally, experiments on specimens cut from different positions in a component were carried out.

### 2.1 Anisotropy and effects of pre-deformation on stress vs. strain curves

In order to characterize the anisotropy of the material, smooth flat tension specimens with three different angles to the rolling direction ( $0^\circ$ ,  $45^\circ$  and  $90^\circ$ ) were manufactured and tested. Fig. 1 shows the engineering stress vs. strain curves of sheet of ZStE340 for three orientations. The  $r$ -values defined as ratio between thickness strain and elongation strain were evaluated. To make use of the assumption of constant volume and to keep the uniaxial loading condition the  $r$ -values were determined only in the loading range before localization (necking). A slight anisotropic effect concerning the deformation behaviour can be recognized from Fig. 1. The fracture strains for rolling direction ( $\theta=0^\circ$ ) are slightly smaller than those for diagonal and transverse direction.

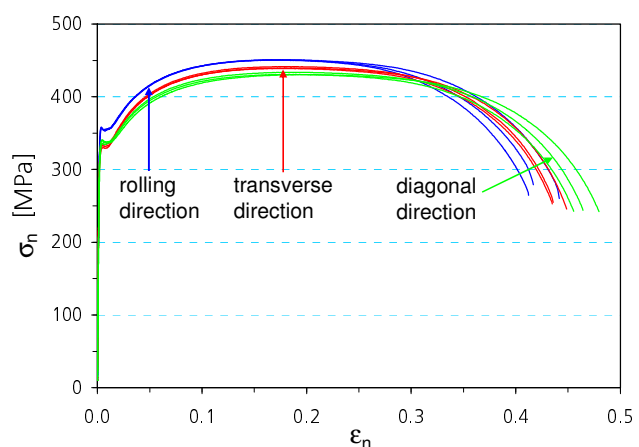


Fig 1: Engineering stress vs. strain curves of sheet of ZStE340 for three orientations

To identify the influence of the forming process on local properties in a real component sub-sized tension specimens were cut from different positions in a steel component made of ZStE340 (Fig. 2). The engineering stress vs. strain curves for different positions are compared with the curves of

specimens from the original sheet (Fig. 3). The distribution of pre-strains in the component is not homogeneous and therefore the flow stress and fracture strain vary in a large range.

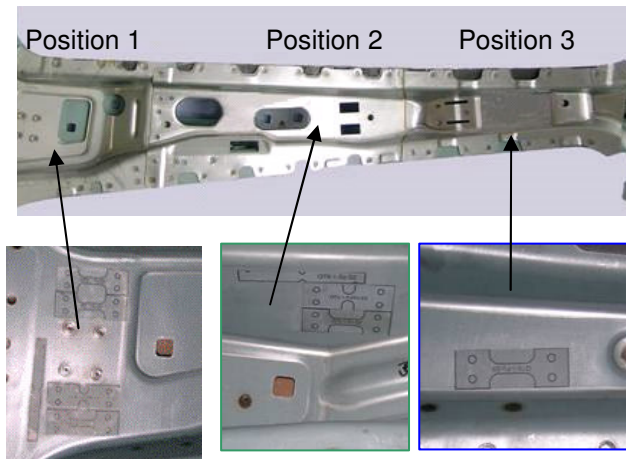


Fig. 2: Component and extraction positions of tension specimens

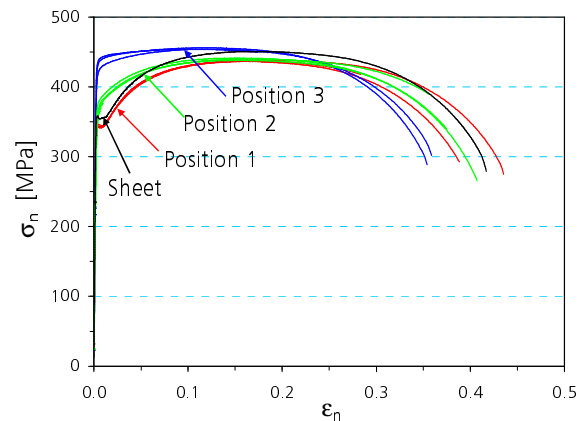
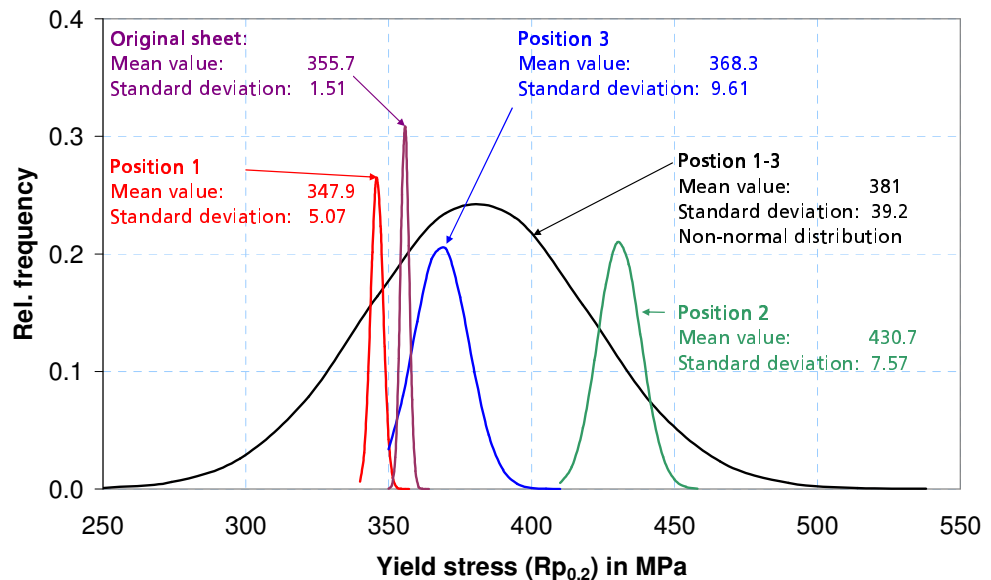


Fig. 3: Engineering stress vs. strain curves from different positions of the component (Fig. 2) compared to original sheet curves

### 2.2 Statistic evaluation of results of tensile tests

The scatter of tensile tests was statistically evaluated. The distributions of yield stress for different test series are shown in Fig. 4. For one test series 3 to 11 specimens were used. The scatter of the yield stress is very small within a test series. However, the values of yield stress between the different positions in the component and the original sheet are remarkably different. This is a clear evidence that the deterministic scatter e.g. position dependence has to be separately treated from the stochastic scatter. In this work the dependence of flow stress on position in the component was determined on the basis of a forming simulation.

Fig 4: Scatter of yield stress in a component manufactured by deep drawing for three different positions in comparison with the data from the original sheet



### 2.3 Influence of triaxiality on the damage behaviour

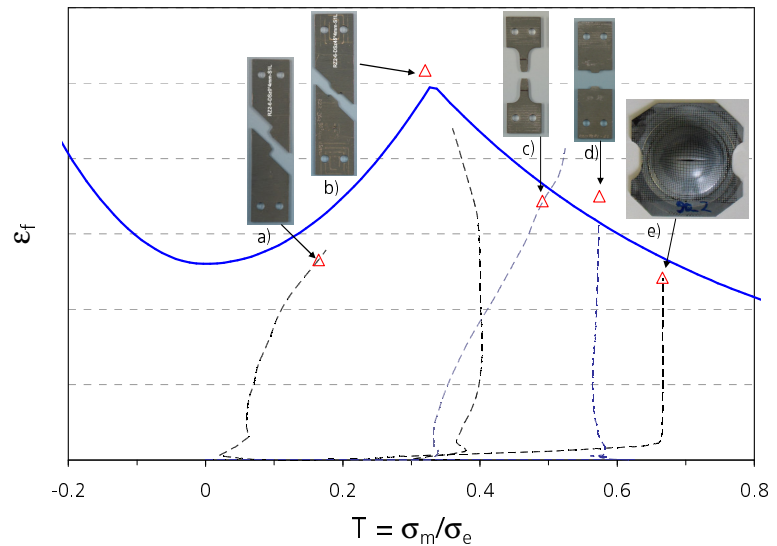
To study the influence of triaxiality on damage behaviour, shear tension tests, smooth tension tests, notched tension tests and biaxial tension tests were performed under static loading (Fig. 5). The triaxiality is defined as the ratio of the mean stress  $\sigma_m$  to the von Mises stress  $\sigma_e$ . The stress triaxiality in the shear tension specimen depends on the angle  $\theta$  between the line connecting both notch tips

and the load line [4]. By increasing the angle  $\theta$  from  $0^\circ$  to  $90^\circ$ , the load type can be varied from pure shear to pure tension. Since local strains and triaxiality are not homogeneous in the specimens due to stress gradients or localization of deformation, FE simulations were performed to determine the local fracture strains and triaxiality. Fig. 5 shows the fracture strains obtained with five different specimens. The values presented by triangle symbols in Fig. 5 were determined by fitting the calculated load vs. displacement curve to the measured one at rupture. Triaxiality changes with increasing loading especially in shear-tension and smooth tension specimens. Fig.5 shows that the fracture strain under shear is lower than that under uniaxial tension for this material.

Fig 5: Fracture strain  $\epsilon_f$  as function of stress triaxiality  $\sigma_m/\sigma_e$  for original sheet of ZStE340 and loading history (dash lines) for different tests

- a) shear tension  $\theta=0^\circ$
- b) shear tension  $\theta=45^\circ$
- c) smooth tension
- d) notched tension with notch radius  $r=1\text{ mm}$
- e) Nakazima biaxial tension

Triangle : experiment + simulation  
 dash line : loading path from simulation  
 blue line : damage curve for simulation



### 3 Damage modelling for simulation of the process chain

Many experiments [5, 6] give evidence that both types of ductile fracture i.e. shear failure and dimple rupture can occur in a metallic component under complex loading. The fracture strain in shear can be below fracture strains at higher triaxialities, which is contrary to the assumption of conventional damage models like Gurson [6] and Johnson-Cook [10]. The problem of the conventional damage models is that they take into account only the micro-mechanism of void growth which is controlled by hydrostatic stress. The micro-mechanisms of shear failure are the initiation of micro-cracks at grain boundaries by shear stress through slipping between neighboring grains and subsequent extension or connection through intergranular boundaries or through transgranular slip bands [7]. Therefore, the damage development under shear is not tied to hydrostatic stress and should be described by deviatoric stresses [6]. A damage concept for shear failure and dimple fracture was developed in [4, 8] based on experimental observations and theoretical analyses in the literature and used in this work in combination with a material model for anisotropic behaviour.

#### 3.1 Material model for anisotropic deformation

To model planar anisotropic deformation behaviour of sheet metals the Barlat-3K model [9] was used for simulations with shell elements. The yield function  $\phi$  is written as

$$\Phi = a |K_1 + K_2|^m + a |K_1 - K_2|^m + (2 - a) |2K_2|^m = 2\sigma_{\text{yield}}^m \quad (1)$$

with

$$K_1 = \frac{\sigma_{xx} + h\sigma_{yy}}{2}, \quad K_2 = \sqrt{\left(\frac{\sigma_{xx} - h\sigma_{yy}}{2}\right)^2 + p^2\sigma_{xy}^2} \quad (2)$$

$\sigma_{\text{yield}}$  denotes the yield stress in the rolling direction (x-direction). The parameters  $m$ ,  $a$ ,  $h$  and  $p$  describe the plastic anisotropy;  $a$ ,  $h$  and  $p$  are obtained through the Lankford parameters  $r_0$ ,  $r_{90}$  and  $r_{45}$ .

### 3.2 Bi-Failure damage model

The damage model used in this work is based on a fracture strain criterion. The fracture strain  $\varepsilon_f$  is defined as a function of the stress triaxiality  $T = \sigma_m / \sigma_e$ . The difference to the Johnson-Cook type fracture criterion [10] is that the fracture strain does not decrease monotonically with increasing triaxiality. The damage curve describing the dependence of fracture strain on triaxiality is divided into two regions for dimple rupture at high triaxialities and shear failure at low triaxialities, as shown in Fig. 5 with the boundary at  $T = 1/3$ . The failure curve proposed by Johnson-Cook (3) is used above a triaxiality  $T_{trans}$  (which is a material parameter and is expected to be about 1/3). The Johnson-Cook model involves three material parameters  $d_1$ ,  $d_2$  and  $d_3$ . An empirical polynomial curve (4) is proposed below  $T_{trans}$  with a minimum at  $T = 0$ .

$$T > T_{trans} \quad \varepsilon_f = (d_1 + d_2 \exp(-d_3 T)) \quad (3)$$

$$T < T_{trans} \quad \varepsilon_f = d_{shear1} + d_{shear2} |T|^{m_2} + d_{shear3} \langle -T \rangle^{m_3} \quad (4)$$

The third term in (4) is introduced to define an asymmetry in the failure strain with respect to the triaxiality, especially to take into account different failure strains in tension and compression, or no failure in compression at all. In equation (4)  $\langle \cdot \rangle$  denote the Macauley brackets which return the argument if positive and zero if negative. The parameters  $d_{shear1}$ ,  $m_2$  and  $m_3$  are material parameters for the shear region  $T < T_{trans}$ . The value  $d_{shear2}$  is set to ensure the continuity of the failure strain function at  $T_{trans}$ . The parameter  $d_{shear3}$  can be determined from the fracture strain under uniaxial compression ( $T = -1/3$ ).

Fracture occurs when the cumulative damage parameter  $D$  defined by (5) reaches the critical value of one. Johnson-Cook [10] proposed a linear damage accumulation. A more general non-linear damage accumulation is used here:

$$\dot{D} = \frac{n}{\varepsilon_f} D^{1-\frac{1}{n}} \dot{\varepsilon}_p \quad (5)$$

$\varepsilon_p$  denotes the equivalent plastic strain and the exponent  $n$  is a parameter controlling damage evolution. For constant  $\varepsilon_f$  the integration of (5) leads to  $D = (\varepsilon_p / \varepsilon_f)^n$ . From a physical point of view a non-linear evolution of damage is reasonable. However, the determination of the  $n$ -value is difficult. For this reason  $n=1$  was used in this work.

The new damage model GISSMO (MAT\_ADD\_EROSION) in LS-DYNA can be calibrated to be the same as this damage model by defining a curve which corresponds to (3) and (4). A detailed description of this model was given by Neukamm et al. [11]. Since the input for the model GISSMO is given by a curve, it offers a large flexibility for describing the form of damage curves. The advantage of the Bi-Failure model is that the damage parameters can be easily fitted using the analytical formulas given above. The Bi-Failure model can be used for a large loading variation based on a limited number of specimen types due to the physical and explicit description of the dependence of the damage parameters on triaxiality.

### 3.3 Simulation of specimen tests

The damage model described above was used to simulate all specimen tests performed in this work. The damage parameters  $d_1$ ,  $d_2$  and  $d_3$  for the region  $T > 1/3$  were determined by fitting the fracture strains of smooth and notched tension and Nakazima specimens. The damage parameters for the range  $T < 1/3$  were obtained by fitting the fracture strains of different shear tests. The sheets of the investigated ZStE340 steel do not show failure under compression. Therefore, a very high value of fracture strain was assumed for uniaxial compression. The damage curve used in this work is given in Fig. 5. To investigate the influence of anisotropy on deformation behaviour of different specimens the simulations were performed with the Barlat and the von Mises flow function in combination with the damage model described in section 3.2.

Fig. 6 compares the engineering stress vs. strain curves for three orientations from experiment and simulation performed with the Barlat model in combination with the Bi-Failure damage model. The orientation dependence of the yield stress was well calculated by the Barlat model with the chosen parameters. The deviation between experiment and simulation gets larger with increasing

deformation. Obviously, the Barlat model cannot fully predict the anisotropic behaviour of the whole deformation. The strains measured at fracture were well calculated by the Bi-Failure model. Fig. 7 compares the measured and calculated normalized force vs. displacement curves of smooth and notched tension specimens. Fig. 8 and Fig. 9 show the measured and calculated load vs. displacement curves of shear tension tests with two specimen geometries ( $\theta=0^\circ$  and  $45^\circ$ ). In all cases the calculated displacements at fracture agree well with experimental results. The Barlat model delivers a better prediction of the force vs. displacement curves for both shear tension tests. The deformed meshes at beginning of rupture are also shown in Fig. 8 and Fig. 9. The damage initiates in the centre of the specimen with  $\theta=0^\circ$  and at the notch root of the specimen with  $\theta=45^\circ$  due to different fractions of shear stresses.

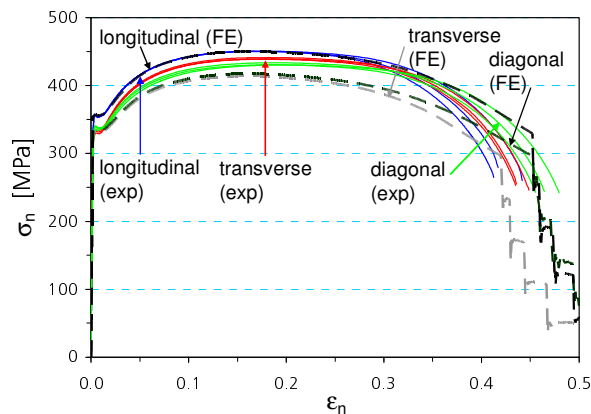


Fig. 6: Measured and calculated engineering stress vs. strain curves for three orientations

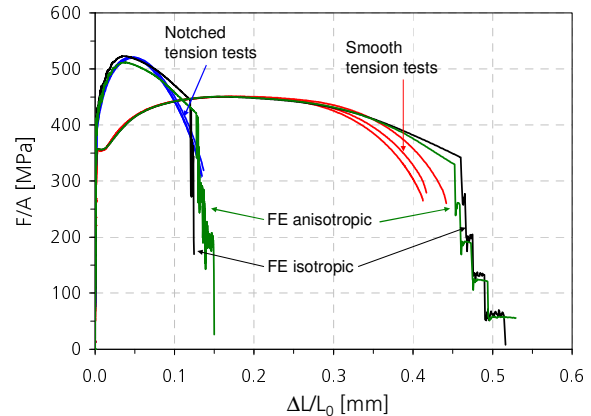


Fig. 7: Measured and calculated normalized force vs. displacement curves for smooth and notched tension specimens

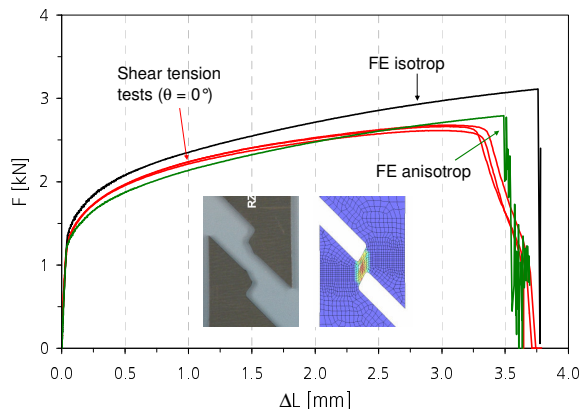


Fig. 8: Measured and calculated force vs. displacement curves of shear tension tests ( $\theta=0^\circ$ )

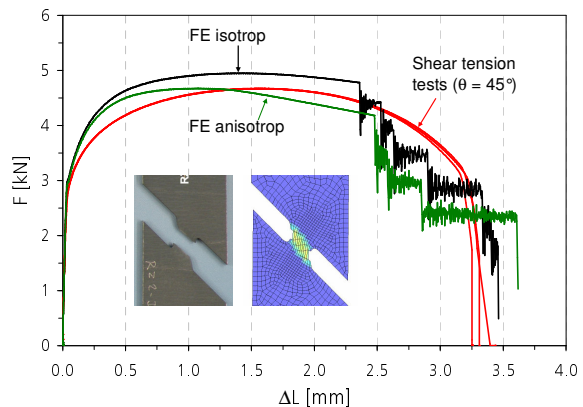


Fig. 9: Measured and calculated force vs. displacement curves of shear tension tests ( $\theta=45^\circ$ )

Fig. 10 compares the measured and calculated load vs. punch displacement curves of Nakazima tests which were performed at IEHK of RWTH Aachen. As shown in Fig. 5 the triaxiality in the Nakazima specimen is nearly  $2/3$  during the whole loading process. This means that the Nakazima specimens with width of 90 mm were loaded under ideal equi-biaxial tension. The simulations show that the friction coefficient  $\mu$  has a large influence on the force, distribution of strains and damage pattern. Since film and fat were applied on the specimen surfaces before experiment, the simulations were conducted under the assumption of free friction between metal sheet and punch. The difference of the numerical results with and without modelling the anisotropy effects is negligible in the case of biaxial loading (Nakazima tests).

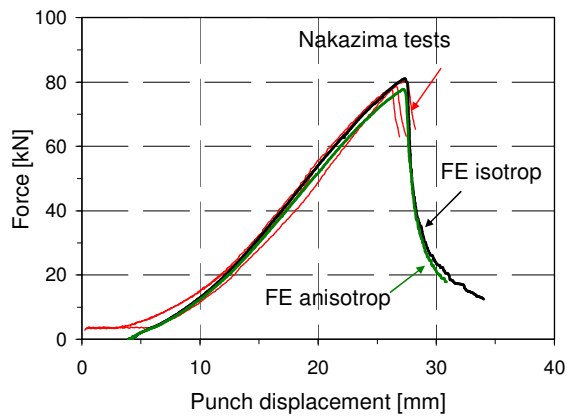


Fig. 10: Measured and simulated force vs. punch displacement curves of Nakazima tests

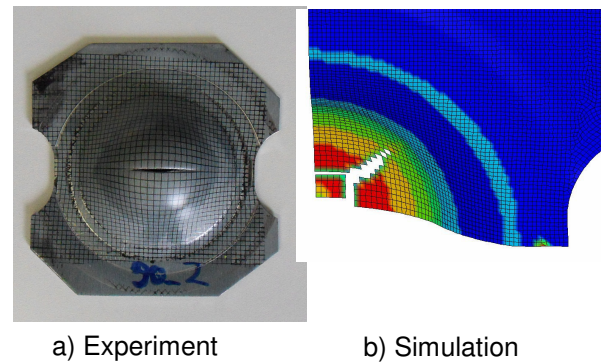


Fig. 11: Damage pattern of Nakazima specimen in experiment and simulation (1/4 model)

## 4 Component and crash simulation

### 4.1 Bending test with superimposed tension

Static tests on the component of ZStE340 manufactured by deep drawing were performed to validate the applied concept for damage modelling. The component was loaded under bending with superimposed global tension to intensify loading. Fig. 12 shows the test set up for the bending test with superimposed tension which was achieved by supporting the component at both ends by revolvable bearings. Fig. 13 shows the measured load vs. displacement curves of three component tests and the deformation of a component at three stages. The peak load at punch displacement of 73 mm is related to the beginning of folding of the component. The crack initiates in one flange of the component at a punch displacement of 137 mm. Finally, the component fails due to crack propagation from flange to the component centre. Bending is the dominant load before reaching the second minimum of the load and after that the superimposed tension is mainly responsible for further deformation.



Fig. 12: Test set up for bending test with superimposed tension on a component

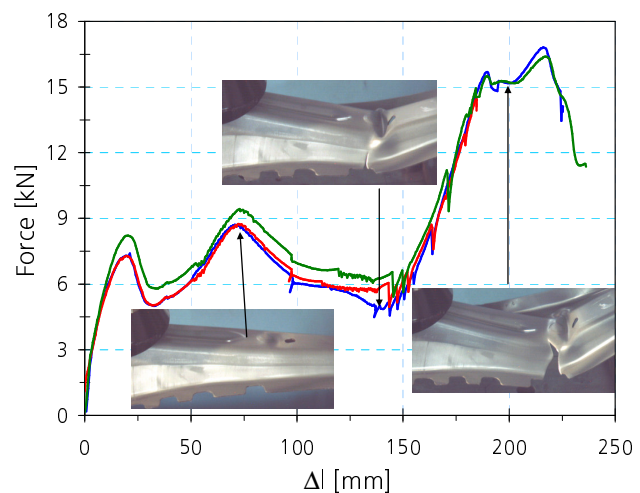


Fig. 13: Measured load vs. displacement curves of component tests with deformation pattern at three stages

### 4.2 Mapping of forming simulation results and modelling of pre-strains

The distributions of pre-strain, pre-damage and sheet thickness calculated from deep-drawing simulation were transferred to a crash model by using the SCAIMapper [12]. The application of a mapping method is necessary, as element sizes for crash simulation are generally coarser than those for forming simulation and geometry deviations between the two models exist due to cutting after deep

drawing. Fig. 14 shows the distribution of equivalent plastic strain mapped from the model for forming simulation onto the model for crash simulation. Sub-sized smooth tension specimens were cut from different positions in the component and tested under static loading to check the results of forming simulation. Fig. 15 compares the engineering stress vs. strain curves of tension specimens cut from the three positions marked in Fig. 14 in comparison with numerical predictions. The corresponding plastic equivalent strain, damage value and sheet thickness calculated by forming simulation were used in the simulation of the tension tests as initial conditions. The measured flow stresses for different positions were well predicted based on the results of forming simulation. The measured reduction of fracture strain caused by pre-deformation agrees with the calculated value in the case of specimen positions a and b. The measured and calculated slopes of the stress vs. strain curves for the specimen position c are completely different. The reason is that the necking of specimen from position c did not occur in the specimen centre but near a boundary of measurement length  $L_0$ . The elongation measured within  $L_0$  does not comprise the whole elongation caused by necking. In the simulation necking takes place in the specimen centre and the whole localisation was taken into account for the evaluation of elongation and engineering strain.

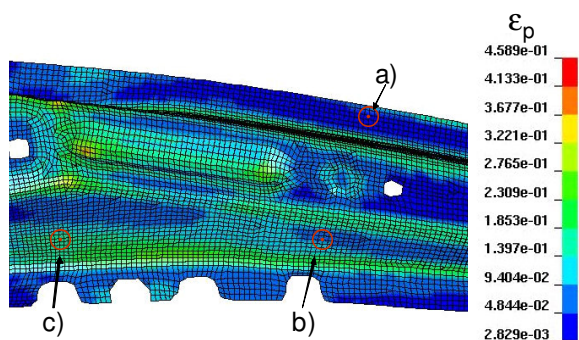


Fig. 14: Distribution of equivalent plastic strain mapped from model for forming simulation onto crash model

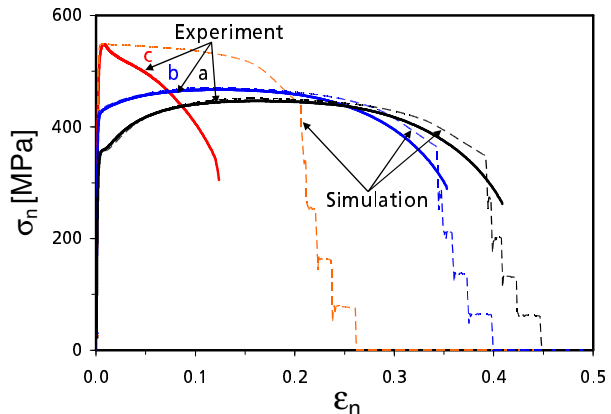


Fig. 15: Engineering stress vs. strain curves of tension specimens cut from the three positions marked in Fig. 14 in comparison with predictions

### 4.3 Modelling of the process chain from deep drawing to crash

The component tests shown in section 4.1 were simulated with the Bi-Failure model and the damage parameters obtained from the original sheet. The mapped distributions of pre-strain, pre-damage and sheet thickness were used as initial values for shell elements. Since damage parameters depend strongly on element size and the crash model of the component consists of elements which are about 8 times larger than the elements in the models for specimen simulations, a calibration method was used to calibrate the mesh size dependence of the damage parameters. A tension test on a large smooth specimen with width of 20 mm and measurement length of 80 mm was simulated with different mesh sizes. The fracture strain for each element size was determined by fitting the measured displacement at fracture. Since the fracture strain under equi-biaxial loading is nearly independent of element size and deep drawing occurs under equi-biaxial loading, the damage parameters for the forming simulation are the same as for the specimen simulations.

The component tests under bending with superimposed tension were simulated with and without taking into account the influence of pre-deformation caused by deep drawing. The calculated damage patterns from both simulations are compared with the experimental results in Fig. 16. With consideration of the pre-deformation from deep-drawing simulation, a good agreement between experiment and simulation was achieved. Without consideration of the forming process, the calculated damage is not sufficient for crack initiation at flange. Damage occurs with increasing loading in the centre of the component which does not agree with experimental observation. Fig. 17 compares the force vs. punch displacement curves from experiments and simulations. The agreement between simulation and testing at small displacements is not satisfying. At the beginning of test rolling of the bearing at the top of the blank occurs and this results in the first maximum at the force-displacement-curve. This complex rolling motion was not in the focus of our comparison. After the rolling motion, bending load is applied to the sheet. The initial crack occurs at a punch displacement of about 100

mm. After the load minimum at punch displacement of 143 mm tensile loading becomes dominant. The component simulation using the initial distributions of pre-strain, pre-damage and thickness reduction mapped from forming simulation delivers a good prediction of the maximum load and of the running of the force vs. displacement curve after the maximum load. The simulation without taking into account the influence of forming process overestimates the load carrying capacity of the component and cannot predict the final failure.

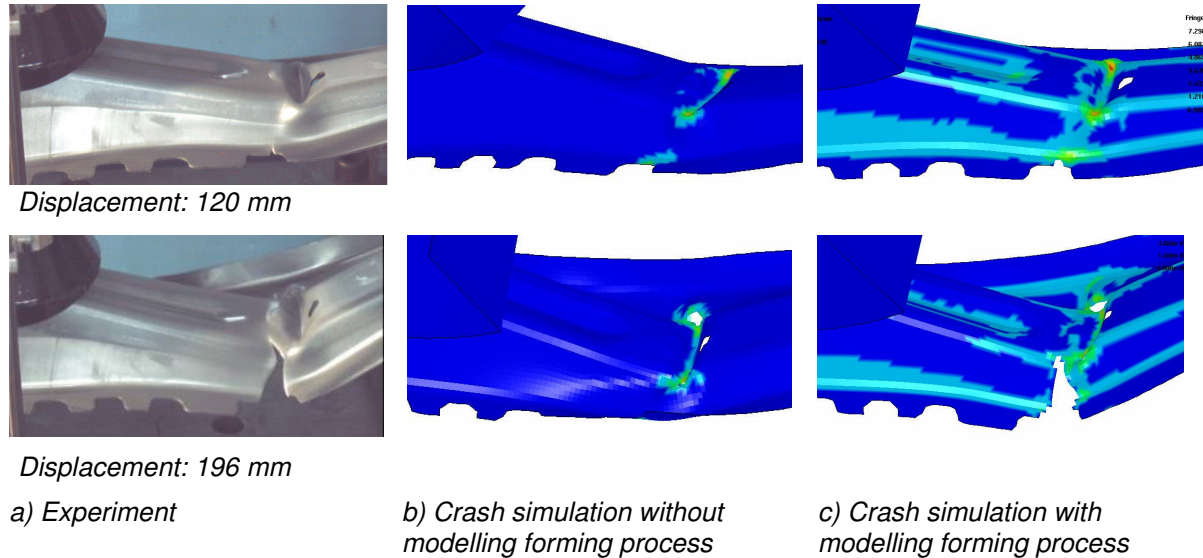
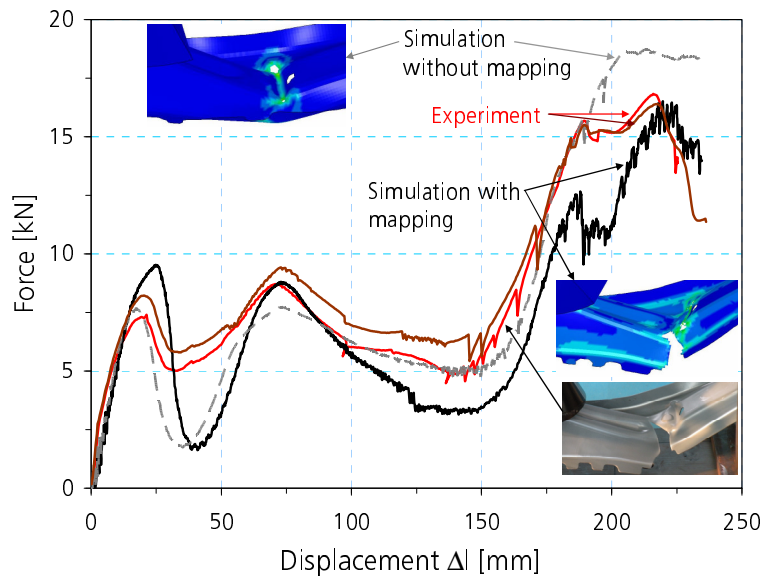


Fig. 16: Damage pattern of a component from experiment and simulation for two load levels

Fig. 17: Measured and calculated load vs. displacement curves of component tests with the corresponding damage patterns



This verified component model with all material parameters was used to quantify the influence of scatter of material data for a systematic stochastic analysis on the basis of the singular value decomposition (SVD) method [3]. This study contains a detailed analysis with 15 design parameters (12 material parameters and 3 process parameters) It was found that the variation of damage parameters has a dominant effect on the numerical results.

## 5 Conclusions

The scatters of material data can be divided into the stochastic and deterministic parts. The variations of flow stress and fracture strain in a component manufactured by deep drawing are not stochastic scatter and can be well determined by forming simulation. The tension tests on specimens from the

original sheet and the component show that the deterministic effect is much greater than the stochastic effect. An integrated simulation from forming to crash is an efficient and reliable method to make a prediction of crash behaviour of an automotive component produced by deep drawing.

A method for the simulation of the process chain from forming to crash was developed and applied for a component made of the steel ZStE340. The main tasks were characterisation and modelling of the influence of triaxiality and loading history on deformation and damage behaviour. The triaxiality for the material characterisation was varied from shear through uniaxial tension to equi-biaxial tension. The influence of loading history on damage behaviour was studied with tension specimens cut from the component. Specimens with different shear-tension ratios were used to characterise damage behaviour between pure shear and tension. The Bi-Failure damage model describing shear and dimple fracture was applied for an integrated simulation from deep drawing to crash. The component simulation with the mapped distributions of pre-strain, pre-damage and sheet thickness shows a good agreement with the experimental results. The simulation without taking into account the influence of pre-deformation and pre-damage cannot predict the damage pattern observed in experiment. This damage concept for the simulation of the process chain was further used for a systematic analysis of additional stochastic effects.

## 6 Literature

- [1] Roux, W., Stander, N., Günther, F., Müllerschön, H.: Stochastic analysis of highly non-linear structures, *Int. J. Numer. Meth. Engng* 2006, 65 1221-1242.
- [2] Günther, F., Müllerschön, H., Roux, W.: Robust design for crash at DaimlerChrysler commercial vehicles CAE, 3. LS-DYNA FORUM 2004, Oct. 14/15, Bamberg.
- [3] Clees, T., Steffes-lai, D.: PRO-CHAIN – Efficient statistical analysis of process chains applied to a forming-to-crash example, 9. LS-DYNA FORUM 2010, 12.-13. Okt. 2010, Bamberg.
- [4] Sun, D.-Z., Andrieux, F., Feucht, M.: Damage modelling of a TRIP steel for integrated simulation from deep drawing to crash, 7th European LS-DYNA Conference, 14.-15. Mai 2009, Salzburg.
- [5] Bao, Y., Wierzbicki, T.: On fracture locus in the equivalent strain and stress triaxiality space, *Int. J. Mech. Sci.*, 2004, 46 (81), 81-98.
- [6] Nahshon, K., Hutchinson, J.W.: Modification of the Gurson Model for shear failure, *Euro. J. Mech. A/Solids*, 2008, 27, 1-17.
- [7] Zhu, H., Zhu, L., Chen, J.H., Lv, X.-F.: Investigation of fracture mechanism of 6063 aluminum alloy under different stress states *Int. J. Fract.*, 2007, 146, 159-172.
- [8] Andrieux, F., Sun, D.-Z.: Damage modelling for simulation of process chain from forming to crash, *Int. J. Mat. Res. (formerly Z. Metallkd.)* 101 (2010) 8, 963-971.
- [9] Barlat, F., Lian, J.: Plastic behaviour and stretchability of sheet metals, *Int. J. of Plasticity*, Vol. 5, 1989, 51-66.
- [10] Johnson, G.R., Cook, W.H.: Fracture characteristics of three metals subjected to various strains, strain rates, temperatures and pressures, *Engineering Fracture Mechanics*, vol.21, No.1, 1985, 31-48.
- [11] Neukamm, F., Feucht, M., Haufe, A.: Fracture characteristics of three metals subjected to various strains, strain rates, temperatures and pressures, 7. LS-DYNA Anwenderforum, 30. Sept.-1. Oct.2008 Bamberg, Germany.
- [12] Helbig, M., Andrieux, F., Steffes-lai, D., Clees, T.: Development of a material model for the process chain forming to crash taking stochastic and deterministic influences into account, ANSYS Conference & 27th CDFEM Users' Meeting 2009, Nov. 18-20, 2009, Leipzig.